

## RESEARCH ARTICLE



# Exploration of Neuroprotective and Retinoprotective Mechanisms of Plumbagin Using Network Pharmacology and Molecular Docking

Kalyani Sakure<sup>1</sup>, Anju Daharia<sup>2</sup>, Alok Singh Thakur<sup>\*2</sup>, Madhulika Pradhan<sup>3</sup>, Hemant Badwaik<sup>4</sup>

<sup>1</sup> Department of Pharmaceutics, Rungta College of Pharmaceutical Sciences and Research, Bhilai, Chhattisgarh, India

<sup>2</sup> Department of Pharmaceutical Chemistry, SRI Shankaracharya Professional University, Bhilai, Chhattisgarh, India

<sup>3</sup> Department of Pharmacy, Rungta International Skills University, Bhilai, Chhattisgarh, India

<sup>4</sup> Department of Pharmacy, SRI Shankaracharya Professional University, Bhilai, Chhattisgarh, India

Publication history: Received on 17<sup>th</sup> January 2026; Revised on 25<sup>th</sup> February 2026; Accepted on 26<sup>th</sup> February 2026

Article DOI: 10.69613/44285k71

**Abstract:** Plumbagin, a naturally occurring naphthoquinone, reported to have significant potential in mitigating neuronal and retinal damage. Study of its pharmacokinetic properties reveals favorable drug-likeness and toxicity profiles, supporting its viability as a therapeutic lead. Target prediction and disease-specific gene retrieval identified 50 common targets at the intersection of plumbagin bioactivity and neurodegenerative pathways. Protein-protein interaction networks highlight STAT3, NFKB1, ITGB1, and HDAC2 as primary hub proteins. These targets are intrinsically linked to cellular survival, inflammatory modulation, and oxidative stress management. Functional enrichment indicated that plumbagin primarily operates via the PI3K-Akt, HIF-1, AGE-RAGE, and Toll-like receptor signaling cascades. Molecular docking simulations further validated these findings, showing good binding affinities for plumbagin with STAT3 (-89.86 kcal/mol) and NFKB1 (-88.86 kcal/mol). These interactions indicate a regulatory role in transcriptional activities essential for neuroprotection. The integration of systems-level network pharmacology with site-specific molecular docking characterizes plumbagin as a multi-target phytochemical scaffold capable of stabilizing neuronal integrity. Such evidence provides a computational foundation for developing novel interventions for neurodegenerative and retinopathic conditions.

**Keywords:** Plumbagin; Neuroprotection; Retinopathy; Network Pharmacology; Molecular Docking.

## 1. Introduction

Plumbagin (5-hydroxy-2-methyl-1,4-naphthoquinone) is a secondary metabolite primarily derived from the roots of the *Plumbago zeylanica* L. plant, a member of the Plumbaginaceae family [1]. Structurally, it is a naphthoquinone derivative characterized by a conjugated quinonoid system that confers high redox activity and electrophilic properties [2]. These chemical attributes enable plumbagin to interact with various cellular nucleophiles and modulate diverse signaling environments. Historically, this phytochemical has been recognized for its broad spectrum of biological activities, including potent antioxidant, anti-inflammatory, antimicrobial, and anticancer properties [3]. Its ability to cross biological barriers and influence intracellular redox status makes it a subject of intense investigation in the field of neurotherapeutics [4].

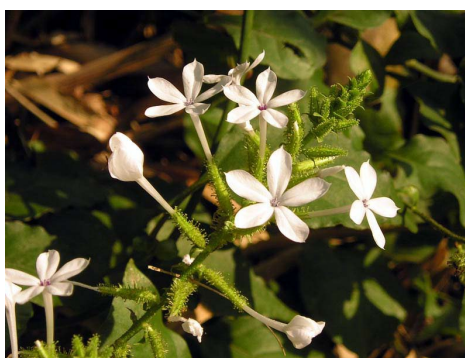


Figure 1. Leaves and Flowers of *Plumbago zeylanica* L.

\* Corresponding author: Alok Singh Thakur

Neurodegenerative disorders and retinopathies share common pathological hallmarks, including chronic inflammation, mitochondrial dysfunction, and excessive production of reactive oxygen species (ROS) [5]. In the central nervous system and the retina, the accumulation of oxidative damage leads to the apoptosis of neurons and retinal ganglion cells (RGCs), eventually resulting in irreversible functional loss [6]. Current therapeutic strategies often focus on single-target interventions; however, the multifactorial nature of these diseases necessitates a more holistic, multi-target approach. Plumbagin has surfaced as a promising candidate due to its capacity to activate endogenous antioxidant defenses, such as the Nrf2/ARE pathway, and suppress pro-inflammatory cascades including the NF- $\kappa$ B signaling axis [7].

The advent of network pharmacology has revolutionized the identification of therapeutic mechanisms by shifting the paradigm from "one drug, one target" to "one drug, multiple targets" [8]. This methodology allows for the visualization of complex interactions between phytochemicals and biological systems, facilitating the discovery of synergistic effects across multiple pathways. Molecular docking provides a structural basis for these interactions, predicting the binding affinity and orientation of ligands within protein active sites [9]. Despite the documented benefits of plumbagin, a gap remains in the systematic mapping of its neuroprotective and retinoprotective targets through integrated computational pipelines. This study utilizes these tools to identify hub genes and signaling pathways that mediate the neuroprotective effects of plumbagin.

---

## 2. Methodology

### 2.1. Molecular Characterization and ADMET Properties

The chemical structure and Canonical SMILES of plumbagin were retrieved from the PubChem database. To evaluate its potential as a therapeutic agent, molecular properties were analyzed using DataWarrior v.6.1.0, and drug-likeness was estimated via the MolSoft platform [10]. Comprehensive pharmacokinetic profiling, including Absorption, Distribution, Metabolism, Excretion, and Toxicity (ADMET), was conducted using SwissADME and ADMETLab 3.0 [11]. The toxicological risks, such as organ toxicity and lethality (LD50), were predicted using the ProTox-II v3.0 server to ensure the safety profile of the compound for future biological applications [12].

### 2.2. Target Identification and Disease Mapping

#### 2.2.1. Prediction of Plumbagin Targets

Potential molecular targets for plumbagin were predicted using the SuperPred tool, which utilizes structural similarity and fragment-based mapping [13]. A probability threshold of  $\geq 65\%$  was implemented to capture a broad range of potential interactions. The resulting targets were standardized using the UniProt database, and their functional annotations were verified through the STRING database for *Homo sapiens*.

#### 2.2.2. Retrieval of Disease-Associated Genes

Genes associated with neurodegenerative diseases and retinal pathologies were harvested from the GeneCards database [14]. The search was refined using the keyword "neurodegenerative diseases," yielding a comprehensive list of proteins involved in disease progression. Only genes with high Relevance Scores and GeneCards Inferred Functionality Scores (GIFtS) were retained to ensure biological significance.

#### 2.2.3. Intersection Analysis

To identify the specific genes through which plumbagin exerts its protective effects, an intersection analysis was performed using Venny 2.1. This step effectively isolated the overlapping genes between the plumbagin-target set and the disease-associated gene set, forming the basis for subsequent network construction [15].

### 2.3. Network Construction and Hub Gene Analysis

#### 2.3.1. Protein-Protein Interaction (PPI) Modeling

The overlapping genes were imported into the STRING 12.0 database to generate a PPI network. A medium confidence score ( $\geq 0.4$ ) was selected to filter the interactions. The resulting network data were exported to Cytoscape v3.10.3 for advanced visualization and topological analysis [16].

### 2.3.2. Identification of Hub Proteins

The CytoHubba plugin within Cytoscape was utilized to rank the nodes based on their degree of connectivity and topological centrality [17]. The top-ranked genes, representing the most critical nodes in the network, were identified as hub genes. These proteins were prioritized for molecular docking validation due to their presumed role in mediating the core therapeutic effects of plumbagin.

### 2.4. Enrichment Analysis (GO and KEGG)

Functional annotation of the target genes was performed using Gene Ontology (GO) and Kyoto Encyclopedia of Genes and Genomes (KEGG) pathway enrichment analysis [18]. The GO analysis categorized genes into Biological Processes (BP), Molecular Functions (MF), and Cellular Components (CC). The KEGG analysis identified the primary signaling pathways involved. Statistical significance was determined using a false discovery rate (FDR) adjusted p-value of <0.05.

### 2.5. Molecular Docking Simulations

#### 2.5.1. Preparation of Ligand and Receptors

The 2D structure of plumbagin was converted into a 3D conformation using Chem3D version 22.2.0. Energy minimization was performed using the MM2 force field to ensure structural stability. The crystal structures of the hub proteins—STAT3 (PDB ID: 6NJS), ITGB1 (PDB ID: 7CEB), NFKB1 (PDB ID: 8TQD), HDAC2 (PDB ID: 4LXZ), and SERPINE1 (PDB ID: 1DVM)—were retrieved from the RSCB Protein Data Bank [19].

#### 2.5.2. Docking Protocol

Simulations were executed using Molegro Virtual Docker (MVD) v6.0. Prior to docking, water molecules were removed, and polar hydrogens were added to the protein structures. A search sphere of 15 Å radius was centered on the known active sites or the co-crystallized ligand coordinates. The MolDock SE algorithm was employed with a grid resolution of 0.30 Å. Each simulation consisted of 10 independent runs with a population size of 50 and 1500 iterations per run to identify the most favorable binding pose based on the MolDock Score and hydrogen bonding energy [20].

**Table 1. Molecular docking grid parameters and structural details of the selected target proteins.**

| Compound ID | Target Protein | PDB ID | Resolution (Å) | Chain        | Volume (Å <sup>3</sup> ) | Surface Area (Å <sup>2</sup> ) | X-Center | Y-Center | Z-Center |
|-------------|----------------|--------|----------------|--------------|--------------------------|--------------------------------|----------|----------|----------|
| A1          | STAT3          | 6NJS   | 2.70           | Single chain | 95.232                   | 270.08                         | -3.19    | 19.07    | 25.87    |
| A2          | ITGB1          | 7CEB   | 2.89           | Chain B      | 44.032                   | 202.24                         | 50.74    | 45.48    | -2.05    |
| A3          | NFKB1          | 8TQD   | 2.80           | Single chain | 16.384                   | 70.40                          | 11.69    | 8.12     | -0.15    |
| A4          | HDAC2          | 4LXZ   | 2.02           | Chain A      | 17.408                   | 62.72                          | 14.82    | -21.14   | -2.61    |
| A5          | SERPINE1       | 1DVM   | 1.85           | Chain A      | 56.832                   | 190.72                         | 10.44    | 18.83    | -41.16   |

## 3. Results

### 3.1. Identification of Overlapping Therapeutic Targets

The initial phase of the network pharmacology assessment involved the cross-referencing of plumbagin-responsive genes with neurodegenerative disease-related targets. Data retrieval from the GeneCard database yielded 1187 genes (92.5%) associated with neurodegenerative conditions. Mapping of plumbagin targets via the STRING 12.0 database identified 46 bioactive-related genes (3.6%). The intersection analysis using Venny 2.1 identified a core set of 50 common genes (3.9%), which likely represent the primary molecular interfaces through which plumbagin exerts its neuroprotective influence.

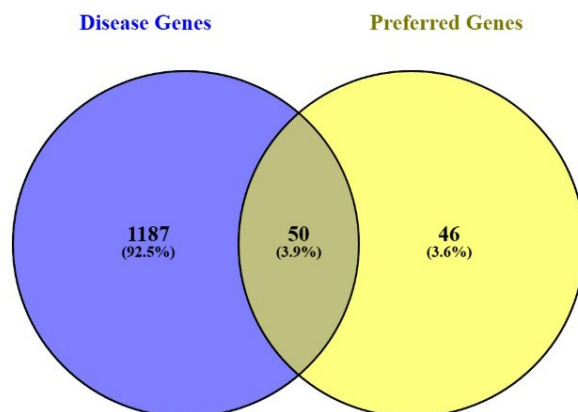


Figure 2. The intersection of neurodegenerative disease genes and plumbagin-responsive targets [8]

### 3.2. Protein-Protein Interaction (PPI) Network Topology

The 50 common genes were utilized to construct a PPI network to visualize the functional interconnectivity of the targets. The resulting network comprised 50 nodes and 109 edges, characterized by a statistically significant enrichment p-value of  $< 9.31e-13$ . The average node degree was calculated as 4.36, while the average local clustering coefficient reached 0.492. These topological parameters suggest a high degree of biological coordination among the identified proteins, indicating that plumbagin influences a consolidated signaling module rather than isolated targets.

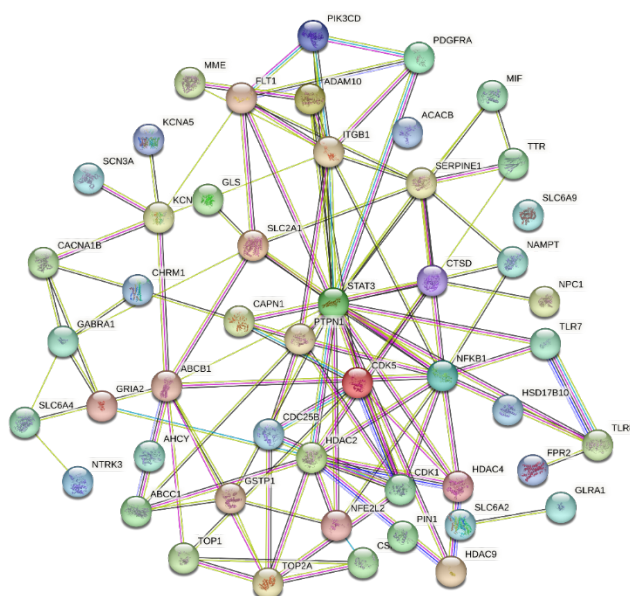


Figure 3. Protein-protein interaction (PPI) network of common target genes

### 3.3. Prioritization of Hub Genes

Topological analysis through the CytoHubba plugin enabled the identification of the top 10 hub genes based on node degree. The ranking revealed STAT3 (degree: 30), ITGB1 (18), NFKB1 (18), HDAC2 (18), SERPINE1 (14), FLT1 (14), CTSD (12), SLC2A1 (12), CDK5 (12), and CDK (10) as the most critical regulators. Among these, STAT3 and NFKB1 emerged as central nodes, suggesting their pivotal roles in the downstream therapeutic effects of plumbagin within the neuro-retinal axis.

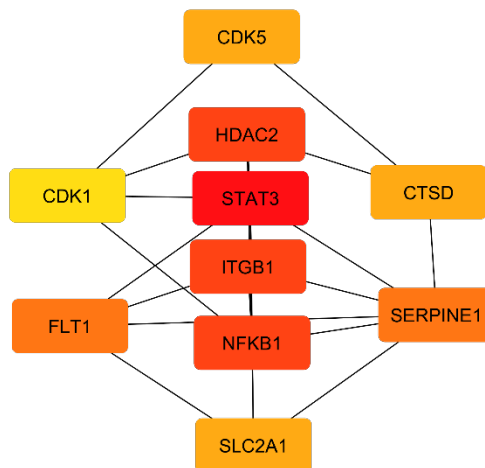


Figure 4. Top 10 hub genes ranked by node degree

### 3.4. Functional Annotation through Gene Ontology

Gene Ontology enrichment categorized the targets into three distinct domains. Biological Process (BP) analysis identified 248 enriched terms, with significant emphasis on cellular processes (GO:0009987), biological regulation (GO:0065007), and metabolic processes (GO:0008152). Specifically, the "cellular process" term encompassed 50 genes with an enrichment strength of 0.12 and an FDR of 0.00023. Cellular Component (CC) analysis identified 57 terms, notably targeting the cytoplasm (GO:0005737) and membrane-bounded organelles (GO:0043227), involving 44 genes with a strength of 0.16 and an FDR of 0.0018. Molecular Function (MF) analysis revealed 39 terms, with protein binding (GO:0005488) showing the highest enrichment, involving 44 genes at a strength of 0.13.

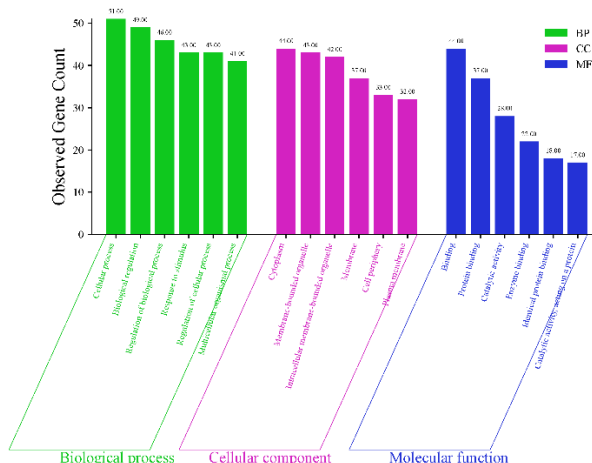


Figure 5. Gene Ontology (GO) functional enrichment analysis

### 3.5. Pathway Enrichment Insights via KEGG

The KEGG pathway analysis mapped the targets to 171 enriched pathways. The top-tier pathways identified for neuroprotection included the HIF-1 signaling pathway (6 genes, fold enrichment: 24.15, p-value: 1.02E-05), the AGE-RAGE signaling pathway in diabetic complications (4 genes, fold enrichment: 17.73, p-value: 0.001007), and the Toll-like receptor signaling pathway (4 genes, fold enrichment: 16.25, p-value: 0.001301). The PI3K-Akt signaling pathway (6 genes, fold enrichment: 7.27, p-value: 0.001766) and general pathways of neurodegeneration (8 genes, fold enrichment: 7.34, p-value: 0.000274) were highlighted as significant therapeutic routes for plumbagin.

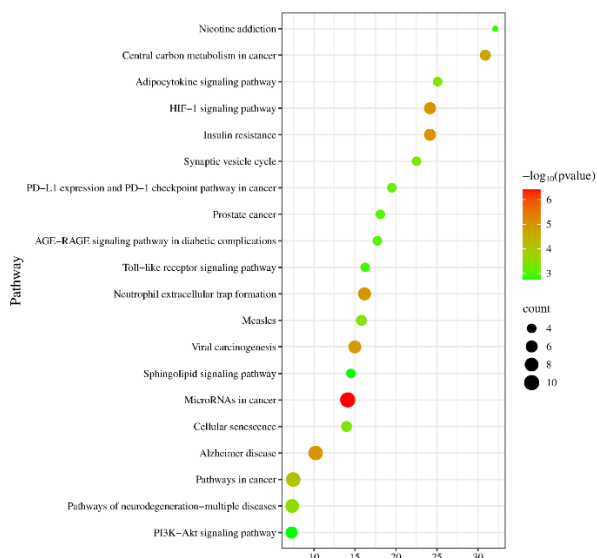


Figure 6. Top 20 KEGG pathway enrichment results shown as a bubble chart generated using the SRplot tool. The X-axis denotes the enrichment score, the Y-axis displays pathway names and codes, and the color gradient of the bubbles indicates the significance level of enrichment

Table 2. KEGG pathway enrichment analysis of plumbagin.

| Pathway Code | Pathway  | Fold Enrichment | p-value  | Gene count | Matching Genes                                |
|--------------|--|-----------------|----------|------------|---|
| hsa05033     | Nicotine addiction                                     | 32.10953        | 0.001301 | 3          | GABRA1, GRIA2, CACNA1B                        |
| hsa05230     | Central carbon metabolism in cancer                    | 30.90353        | 1.76E-05 | 5          | GLS, NTRK3, PDGFRA, PIK3CD, SLC2A1            |
| hsa04920     | Adipocytokine signaling pathway                        | 25.07601        | 0.000374 | 4          | ACACB, NFKB1, SLC2A1, STAT3                   |
| hsa04066     | HIF-1 signaling pathway                                | 24.15579        | 1.02E-05 | 6          | FLT1, NFKB1, SERPINE1, PIK3CD, SLC2A1, STAT3  |
| hsa04931     | Insulin resistance                                     | 24.15579        | 1.02E-05 | 6          | ACACB, NFKB1, PIK3CD, PTPN1, SLC2A1, STAT3    |
| hsa04721     | Synaptic vesicle cycle                                 | 22.50411        | 0.000486 | 4          | SLC6A2, SLC6A4, SLC6A9, CACNA1B               |
| hsa05235     | PD-L1 expression and PD-1 checkpoint pathway in cancer | 19.50356        | 0.000793 | 4          | CSNK2B, NFKB1, PIK3CD, STAT3                  |
| hsa05215     | Prostate cancer  | 18.09609        | 0.000992 | 4          | GSTP1, NFKB1, PDGFRA, PIK3CD                  |
| hsa04933     | AGE-RAGE signaling pathway in diabetic complications   | 17.73051        | 0.001007 | 4          | NFKB1, SERPINE1, PIK3CD, STAT3                |
| hsa04620     | Toll-like receptor signaling pathway                   | 16.25297        | 0.001301 | 4          | NFKB1, TLR7, TLR8, PIK3CD                     |
| hsa04613     | Neutrophil extracellular trap formation                | 16.16743        | 1.02E-05 | 7          | FPR2, HDAC2, NFKB1, TLR7, TLR8, PIK3CD, HDAC9 |
| hsa05162     | Measles  | 15.78526        | 0.000338 | 5          | CSNK2B, NFKB1, TLR7, PIK3CD, STAT3            |

| Pathway Code | Pathway   | Fold Enrichment | p-value  | Gene count | Matching Genes  |
|--------------|---|-----------------|----------|------------|---|
| hsa05203     | Viral carcinogenesis                            | 14.98445        | 1.42E-05 | 7          | HDAC2, NFKB1, PIK3CD, STAT3, HDAC9, HDAC4, CDK1                       |
| hsa04071     | Sphingolipid signaling pathway                  | 14.50678        | 0.001766 | 4          | CTSD, ABCC1, NFKB1, PIK3CD  |
| hsa05206     | MicroRNAs in cancer                             | 14.1103         | 3.88E-07 | 10         | GLS, HDAC2, ABCC1, NFKB1, PDGFRA, ABCB1, PIK3CD, STAT3, HDAC4, CDC25B |
| hsa04218     | Cellular senescence                             | 13.97548        | 0.000486 | 5          | NFKB1, SERPINE1, PIK3CD, CAPN1, CDK1                                  |
| hsa05010     | Alzheimer disease                               | 10.20535        | 1.02E-05 | 9          | ADAM10 CDK5 CHRM1 CSNK2B HSD17B10 MME NFKB1 PIK3CD CAPN1              |
| hsa05200     | Pathways in cancer                              | 7.46592         | 7.24E-05 | 9          | GSTP1, HDAC2, ITGB1, NFE2L2, NFKB1, PDGFRA, PIK3CD, SLC2A1, STAT3     |
| hsa05022     | Pathways of neurodegeneration-multiple diseases | 7.344438        | 0.000274 | 8          | CDK5, CHRM1, CSNK2B, GRIA2, HSD17B10, NFKB1, CACNA1B, CAPN1           |
| hsa04151     | PI3K-Akt signaling pathway                      | 7.273429        | 0.001766 | 6          | CHRM1, FLT1, ITGB1, NFKB1, PDGFRA, PIK3CD                             |

### 3.6. Molecular Docking and Binding Affinity

The binding stability of plumbagin against the prioritized hub proteins was validated through molecular docking. The MolDock scores ranged from -77.898 kcal/mol to -89.863 kcal/mol. STAT3 (A1) exhibited the highest affinity with a score of -89.863 kcal/mol, forming three hydrogen bonds with Gln141 (2.68 Å), Arg246 (2.83 Å), and Leu263 (2.91 Å). NFKB1 (A3) showed a score of -88.861 kcal/mol, characterized by hydrogen bonding at Leu99 (3.35 Å) and His109 (3.31 Å and 2.88 Å). Other interactions included ITGB1 (-86.206 kcal/mol), HDAC2 (-81.342 kcal/mol), and SERPINE1 (-77.898 kcal/mol).

**Table 3. Molecular docking scores and hydrogen bond parameters for plumbagin-target interactions**

| Code | Target Protein | MolDock Score (kcal/mol) | H-Bond (kcal/mol) | No. of H-bonds | H-bond Interaction | H-Bond Distance No. of H-Bond (Å) | No. of S-bonds | S-bond Interaction                                    |
|------|----------------|--------------------------|-------------------|----------------|--------------------|-----------------------------------|----------------|---|
| A1   | STAT3          | -89.863                  | -3.6822           | 3              | Gln141             | 2.68                              | 3              | Gln141, Cys259, Leu263                                |
|      |                |                          |                   |                | Arg246             | 2.83                              |                |   |
|      |                |                          |                   |                | Leu263             | 2.91                              |                |   |
| A2   | ITGB1          | -86.206                  | -2.4509           | 3              | Asn839             | 2.21                              | 1              | Asn839  |
|      |                |                          |                   |                | Lys838             | 2.63                              |                |   |
|      |                |                          |                   |                | Lys903             | 3.12                              |                |   |
| A3   | NFKB1          | -88.861                  | -4.3349           | 3              | Leu99              | 3.35                              | 13             | Gln98, Leu108, His109, Gly121, Ile122, Arg156, Ala160 |
|      |                |                          |                   |                |                    | 3.31                              |                |   |
|      |                |                          |                   |                | His109             | 2.88                              |                |   |
| A4   | HDAC2          | -81.342                  | -8.2138           | -              | -                  | -                                 | 2              | Gly154, His183  |
| A5   | SERPINE1       | -77.898                  | -1.9534           | 1              | Val23              | 2.45                              | -              | -   |

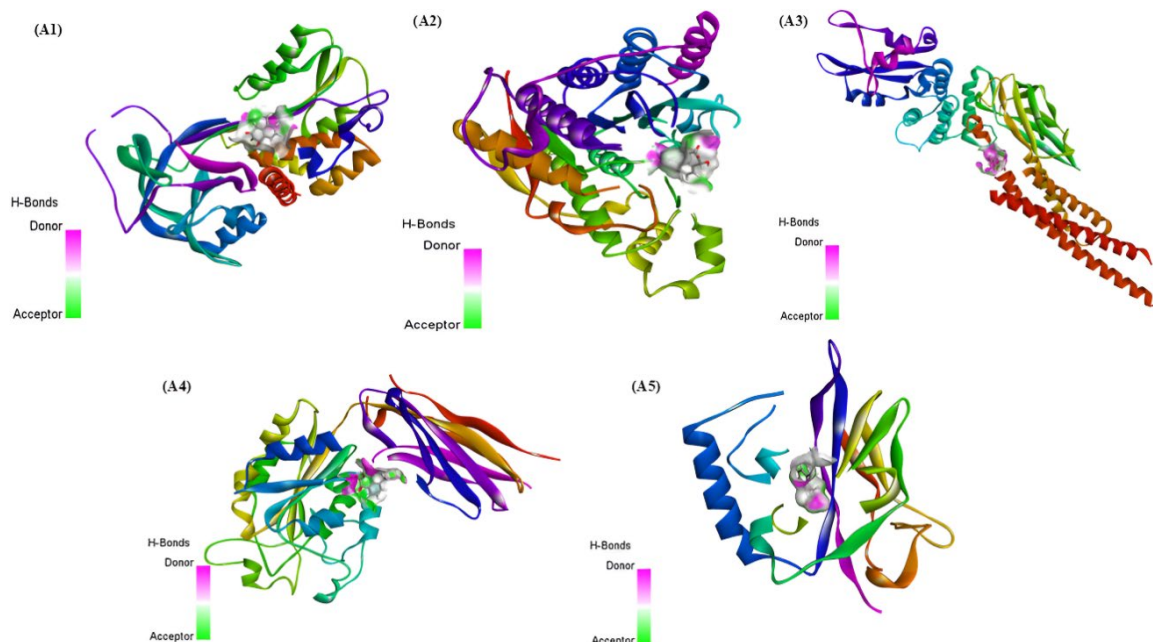


Figure 7. 3D docking poses of plumbagin within protein active sites

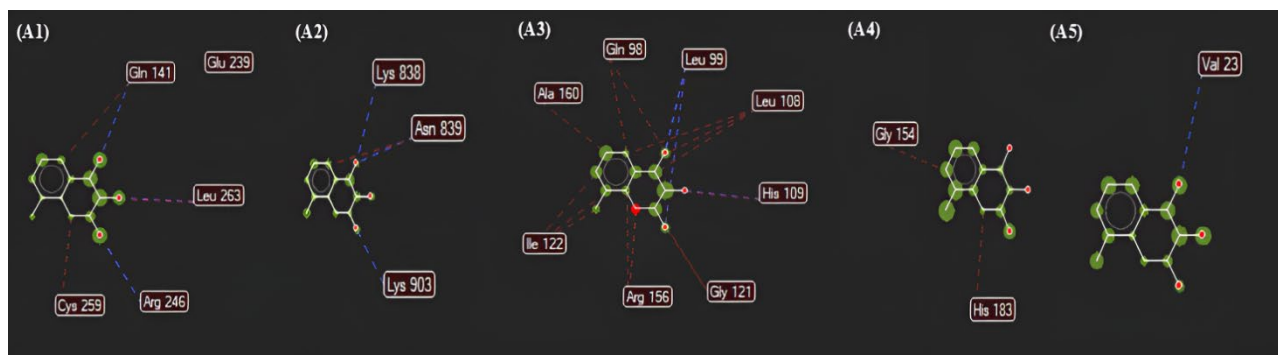


Figure 8. Protein-ligand interaction of the plumbagin with selected target proteins (A1) 6NJS, (A2) 7CEB, (A3) 8TQD, (A4) 4LXZ, (A5) 1DVM. The blue dotted lines indicate the H-bond interaction with the ligand, while the red dotted line represents the S-bond interaction

#### 4. Discussion

The identification of STAT3 as the primary hub gene suggests that plumbagin utilizes the JAK/STAT signaling axis to promote neuroprotection. STAT3 is a crucial regulator of astrocytic activity and microglial responses; its activation by plumbagin may facilitate the suppression of pro-inflammatory cytokines such as TNF- $\alpha$  and IL-1 $\beta$ , thereby reducing the neuroinflammatory burden in glaucomatous and neurodegenerative conditions [21, 22]. In retinal tissues, STAT3 exerts anti-angiogenic effects and preserves retinal ganglion cell integrity by mitigating vascular leakage and oxidative damage [30]. Similarly, the high connectivity of ITGB1 highlights the importance of cell-matrix interactions in neuronal survival. Plumbagin likely modulates ITGB1-mediated PI3K/Akt and MAPK/ERK signaling to enhance synaptic plasticity and inhibit apoptotic pathways under environmental stress [23, 24].

Plumbagin's interaction with NFKB1 and HDAC2 points toward a dual strategy of transcriptional and epigenetic modulation. By binding strongly to NFKB1 (-88.861 kcal/mol), plumbagin disrupts the nuclear translocation of p65/p50 heterodimers, which prevents the over-activation of inflammatory gene expression in retinal neurons [25, 26]. Simultaneously, the interaction with HDAC2 suggests an epigenetic mechanism for restoring synaptic function. HDAC2 is known to negatively regulate genes associated with memory and learning; its modulation by plumbagin could potentially alleviate cognitive and functional deficits in neurodegenerative pathologies [27, 28]. The involvement of SERPINE1 (PAI-1) indicates that plumbagin may stabilize the extracellular matrix, preventing the proteolytic degradation that often precedes neuronal loss [29].

Functional enrichment data corroborate the role of plumbagin in neutralizing oxidative insults via the Nrf2-ARE signaling cascade. Plumbagin increases the nuclear localization of Nrf2, stimulating the production of antioxidant enzymes such as glutathione-S-transferase (GST) and heme oxygenase-1 (HO-1) [30, 31]. This antioxidant response is particularly vital in the context of diabetic retinopathy, where the AGE-RAGE signaling pathway triggers chronic oxidative stress and vascular dysfunction. By inhibiting AGE-RAGE-mediated NF- $\kappa$ B activation, plumbagin prevents the structural disorganization of photoreceptors and maintains mitochondrial bioenergetic efficiency [32, 33].

The integrated computational approach shows that plumbagin functions as a pleiotropic agent targeting multiple checkpoints in neurodegenerative and retinopathic cascades. The high binding affinities observed for STAT3 and NFKB1 validate the network-predicted importance of these proteins in inflammatory control. Moreover, the enrichment of the PI3K-Akt and Toll-like receptor pathways suggests that plumbagin provides a comprehensive defensive mechanism against apoptosis and microglial over-activation. These results establish a robust scientific rationale for the further development of plumbagin-based therapeutics in managing retinal ganglion cell loss and associated neurological disorders.

---

## 5. Conclusion

The integration of network pharmacology and molecular docking reveals that plumbagin possesses substantial neuroprotective and retinoprotective capabilities, primarily driven by its multi-target interaction profile. By modulating essential hub proteins such as STAT3, NFKB1, ITGB1, and HDAC2, plumbagin addresses the core pathological drivers of neurodegeneration and glaucomatous damage. These interactions facilitate the suppression of oxidative stress and chronic inflammation through the regulation of the PI3K-Akt, AGE-RAGE, and Toll-like receptor signaling pathways. Computational validation through molecular docking confirms high-affinity binding, particularly with transcriptional regulators, indicating that plumbagin can stabilize neuronal architecture and bioenergetics. These findings characterize plumbagin as a promising phytochemical scaffold for the structural optimization of novel neuroprotective agents. Future scope of this work includes utilizing *in vivo* models to apply this systemic information into clinical therapeutic regimens for ocular and neurological disorders.

---

## References

- [1] Kavi Kishor PB, Thaddi BN, Guddimalli R, Nikam TD, Sambasiva Rao KR, Mukhopadhyay R, et al. The Occurrence, Uses, Biosynthetic Pathway, and Biotechnological Production of Plumbagin, a Potent Antitumor Naphthoquinone. *Molecules*. 2025;30(7):1618.
- [2] Sand JM, Hafeez BB, Jamal MS, Witkowsky O, Siebers EM, Fischer J, et al. Plumbagin (5-hydroxy-2-methyl-1,4-naphthoquinone), isolated from *Plumbago zeylanica*, inhibits ultraviolet radiation-induced development of squamous cell carcinomas. *Carcinogenesis*. 2012;33(1):184-90.
- [3] Hernández-Muñoz LS, Gómez M, González FJ, González I, Frontana C. Towards a molecular-level understanding of the reactivity differences for radical anions of juglone and plumbagin: an electrochemical and spectroelectrochemical approach. *Organic & Biomolecular Chemistry*. 2009;7(9):1896-903.
- [4] Yin Z, Zhang J, Chen L, Guo Q, Yang B, Zhang W, et al. Anticancer effects and mechanisms of action of plumbagin: review of research advances. *BioMed Research International*. 2020;2020:6940953.
- [5] Fan Gaskin JC, Shah MH, Chan EC. Oxidative stress and the role of NADPH oxidase in glaucoma. *Antioxidants*. 2021;10(2):238.
- [6] Ou K, Li Y, Liu L, Li H, Cox K, Wu J, et al. Recent developments of neuroprotective agents for degenerative retinal disorders. *Neural Regeneration Research*. 2022;17(9):1919-28.
- [7] Son TG, Camandola S, Arumugam TV, Cutler RG, Telljohann RS, Mughal MR, et al. Plumbagin, a novel Nrf2/ARE activator, protects against cerebral ischemia. *Journal of Neurochemistry*. 2010;112(5):1316-26.
- [8] Xie E, Nadeem U, Xie B, D'Souza M, Sulakhe D, Skondra D. Using computational drug-gene analysis to identify novel therapeutic candidates for retinal neuroprotection. *International Journal of Molecular Sciences*. 2022;23(20):12648.
- [9] Jakhar R, Dangi M, Khichi A, Chhillar AK. Relevance of molecular docking studies in drug designing. *Current Bioinformatics*. 2020;15(4):270-8.
- [10] Sampat G, Suryawanshi SS, Palled MS, Patil AS, Khanal P, Salokhe AS. Drug likeness screening and evaluation of physicochemical properties of selected medicinal agents by computer aided drug design tools. *Adv Pharmacol Pharm*. 2022;10(4):234-46.

- [11] Fu L, Shi S, Yi J, Wang N, He Y, Wu Z, et al. ADMETlab 3.0: an updated comprehensive online ADMET prediction platform enhanced with broader coverage, improved performance, API functionality and decision support. *Nucleic Acids Research*. 2024;52(W1):W422-31.
- [12] Banerjee P, Eckert AO, Schrey AK, Preissner R. ProTox-II: a webserver for the prediction of toxicity of oral endpoints of small molecules. *Nucleic Acids Research*. 2018;46(W1):W257-63.
- [13] Nickel J, Gohlke BO, Erehman J, Banerjee P, Rong WW, Goede A, et al. SuperPred: update on drug-target prediction and therapeutic indication forecasting. *Nucleic Acids Research*. 2014;42(W1):W26-31.
- [14] Stelzer G, Rosen N, Plaschkes I, Zimmerman S, Twik M, Fishilevich S, et al. The GeneCards Suite: From Gene Data Mining to Disease Genome Sequence Analysis. *Current Protocols in Bioinformatics*. 2016;54(1):1.30.1-1.30.33.
- [15] Oliveros JC. Venny. An interactive tool for comparing lists with Venn's diagrams. 2007. [Available from: <https://bioinfogp.cnb.csic.es/tools/venny/index.html>].
- [16] Shannon P, Markiel A, Ozier O, Baliga NS, Wang JT, Ramage D, et al. Cytoscape: a software environment for integrated models of biomolecular interaction networks. *Genome Research*. 2003;13(11):2498-504.
- [17] Chin CH, Chen SH, Wu HH, Ho CW, Ko MT, Lin CY. cytoHubba: identifying hub objects and sub-networks from complex interactomes. *BMC Systems Biology*. 2014;8(Suppl 4):S11.
- [18] Kanehisa M, Furumichi M, Sato Y, Kawashima M, Ishiguro-Watanabe M. KEGG for taxonomy-based analysis of pathways and genomes. *Nucleic Acids Research*. 2023;51(D1):D587-92.
- [19] Burley SK, Bhikadiya C, Bi C, Bittrich S, Chen L, Crichlow GV, et al. RCSB Protein Data Bank: powerful new tools for exploring 3D structures of biological macromolecules for basic and applied research and education in fundamental biology, biomedicine, biotechnology, and energy. *Nucleic Acids Research*. 2021;49(D1):D437-51.
- [20] Thomsen R, Christensen MH. MolDock: a new technique for high-accuracy molecular docking. *Journal of Medicinal Chemistry*. 2006;49(11):3315-21.
- [21] Guo X, Jiang C, Chen Z, Wang X, Hong F, Hao D. Regulation of the JAK/STAT signaling pathway in spinal cord injury: an updated review. *Frontiers in Immunology*. 2023;14:1276445.
- [22] Ageeva T, Rizvanov A, Mukhamedshina Y. NF- $\kappa$ B and JAK/STAT signaling pathways as crucial regulators of neuroinflammation and astrocyte modulation in spinal cord injury. *Cells*. 2024;13(7):581.
- [23] Ou K, Li Y, Liu L, Li H, Cox K, Wu J, et al. Recent developments of neuroprotective agents for degenerative retinal disorders. *Neural Regeneration Research*. 2022;17(9):1919-28.
- [24] Yan L, Cui Z. Integrin  $\beta$ 1 and the repair after nervous system injury. *European Neurology*. 2023;86(1):2-12.
- [25] Zhang X, Gao L, Wang Y, Meng Q, Bai M, Xu D, et al. The potential and therapeutic advances of the integrin family in neurological disorders. *Neural Regeneration Research*. 2024. doi:10.4103/1673-5374.391218.
- [26] Su C, Mo J, Dong S, Liao Z, Zhang B, Zhu P. Integrin  $\beta$ -1 in disorders and cancers: molecular mechanisms and therapeutic targets. *Cell Communication and Signaling*. 2024;22(1):71.
- [27] Singh S, Singh TG. Role of nuclear factor kappa B (NF- $\kappa$ B) signalling in neurodegenerative diseases: a mechanistic approach. *Current Neuropharmacology*. 2020;18(10):918-35.
- [28] Fanaro GB, Marques MR, Calaza KD, Brito R, Pessoni AM, Mendonça HR, et al. New insights on dietary polyphenols for the Management of Oxidative Stress and Neuroinflammation in diabetic retinopathy. *Antioxidants*. 2023;12(6):1237.
- [29] Ahmad Ganai S, Ramadoss M, Mahadevan V. Histone Deacetylase (HDAC) Inhibitors-emerging roles in neuronal memory, learning, synaptic plasticity and neural regeneration. *Current Neuropharmacology*. 2016;14(1):55-71.
- [30] Fan J, Alsarraf O, Dahrouj M, Platt KA, Chou CJ, Rice DS, et al. Inhibition of HDAC2 protects the retina from ischemic injury. *Investigative Ophthalmology & Visual Science*. 2013;54(6):4072-80.
- [31] Narayana K. SERPINE1/PAI-1 role on blood flow, stalling and vessel width in stroke [Doctoral dissertation]. 2023.
- [32] Catalani E, Del Quondam S, Brunetti K, Cherubini A, Bongiorno S, Taddei AR, et al. Neuroprotective role of plumbagin on eye damage induced by high-sucrose diet in adult fruit fly *Drosophila melanogaster*. *Biomedicine & Pharmacotherapy*. 2023;166:115298.
- [33] Son TG, Camandola S, Arumugam TV, Cutler RG, Telljohann RS, Mughal MR, et al. Plumbagin, a novel Nrf2/ARE activator, protects against cerebral ischemia. *Journal of Neurochemistry*. 2010;112(5):1316-26.